Serially-Concatenated LDGM codes for MIMO channels

Francisco J. Vázquez-Araújo, Miguel González-López, *Member, IEEE*, Luis Castedo, *Member, IEEE*, Javier Garcia-Frias, *Member, IEEE*

Abstract

We investigate the ability of Serially-Concatenated Low Density Generator Matrix (SCLDGM) codes to approach the capacity of ergodic Multiple-Input Multiple-Output (MIMO) channels. First, we explain how to design good SCLDGM codes using EXtrinsic Information Transfer (EXIT) analysis and optimum detection. However, optimum detection becomes unfeasible in many cases of practical interest where the number of transmitting antennas and/or the number of bits per constellation symbol is large. In this case, we resort to List Sphere Detection (LSD), considering two versions: Maximum Likelihood (ML) and Maximum *A Posteriori* (MAP). Again, we use EXIT analysis to obtain good SCLDGM codes for these specific LSD versions. We provide examples of optimized rate $1/2$ SCLDGM codes and show that they perform within 1 dB from the theoretical capacity limit for a large number of antenna configurations and modulation formats. Finally, we discuss how to iteratively improve channel estimation using the soft information computed during the decoding process. We also show how the complexity of channel estimation is reduced by utilizing the candidate list calculated by the LSD.

This work has been supported by Xunta de Galicia, Ministerio de Educación y Ciencia of Spain and FEDER funds of the European Union under grants number PGIDT05PXIC10502PN and TEC2004-06451-C05-01. This work has been prepared through collaborative participation in the Communications and Networks Consortium sponsored by the U.S. Army Research Laboratory under the Collaborative Technology Alliance Program, Cooperative Agreement DAAD19-01-2-0011. The U.S. Government is authorized to reproduce and distribute reprints for Government purposes not withstanding any copyright notation thereon.

This paper was presented in part at the 2006 IEEE Workshop on Signal Processing Advances in Wireless Communications (SPAWC 2006).

Francisco J. Vázquez-Araújo, Miguel González-López and Luis Castedo are with the Departamento de Electrónica y Sistemas, Universidad de A Coruña. e-mail: {fjvazquez,mgonzalezlopez,luis}@udc.es

Javier Garcia-Frias is with the Department of Electrical and Computer Engineering, University of Delaware. e-mail: jgarcia@ee.udel.edu

I. INTRODUCTION

The development of channel codes able to approach the theoretical limits of wireless channels has been an active area of research during the last decade. The basic premise of capacity-achieving codes is to produce long, random-like codewords that resemble Shannon's idea of random coding. So far, Turbo [1] and Low Density Parity Check (LDPC) codes [2], [3] constitute the most prominent examples of capacity-approaching codes. More specifically, it has been shown [4] that LDPC codes are able to approach the capacity of the BIAWGN (Binary Input Additive White Gaussian Noise) channel within a small fraction of a dB. LDPC codes also exhibit an extraordinary good performance when transmitting over Single-Input Single-Output (SISO) channels (either AWGN or Rayleigh) using non-binary modulations [5], [6].

The utilization of Turbo and LDPC codes for transmission over MIMO channels has been studied in [7], [8], [9], [10], [11], among others. Unlike Turbo codes, the main problem of using LDPC codes is their rather high encoding complexity. Several subclasses of LDPC codes with reduced encoding complexity have been proposed, such as Block-LDPC [12], Low-Density Generator Matrix (LDGM) [13] and Repeat-Accumulate (RA) [14]. Block-LDPC codes have been recently adopted in the IEEE 802.16e [15] and IEEE 802.11n [16] standards but their aim is not to approach the ergodic capacity limit: they are specifically designed for short lengths and for minimizing hardware implementation requirements. Low-Density Generator Matrix (LDGM) codes are a class of LDPC codes whose generator matrix is large and random but sparse. Due to their poor minimum distance, LDGM codes are asymptotically bad [17]: they exhibit error-floors independent of the block length. On the other hand, they present a very good convergence threshold so, in practice, they are useful if we utilize techniques to reduce the error floor to a certain level of Bit-Error-Rate (BER) [17], [18]. RA codes reduce the error floor by serially concatenating an LDGM code with an accumulator. The performance of RA codes is rather dependent on the code degree profile: Irregular RA (IRA) codes [19] exhibit a much better performance than their regular counterparts. IRA codes are also attractive for practical implementations and, as an example, they are being used in the second generation standard for satellite digital video broadcasting (DVB-S2) [20]. The error-floor can also be lowered by using an outer code that takes care of the residual errors from the LDGM code [17]. Due to the fact that the number of errors per block to be corrected is very low, it suffices to use a high-rate

code for this task. Since precisely the performance of high-rate LDGM codes is rather good, it is natural to consider the serial concatenation of an outer high-rate LDGM code with an inner LDGM code close to the desired rate. The overall scheme, denominated Serially-Concatenated LDGM (SCLDGM), mantains a good convergence threshold with an error-floor low enough for practical applications [17], [18], [21].

Similarly to LDPC codes, SCLDGM codes may be designed using EXtrinsic Information Transfer (EXIT) charts [10] or Density Evolution (DE) [22]. EXIT charts are less computationally demanding although they cannot be applied in so many cases as DE. As an example, EXIT charts have been applied to find good systematic IRA codes for SISO systems and non-systematic IRA codes for MIMO [23], whereas for the design of systematic IRA codes for MIMO it has been necessary to resort to the DE method [24]. EXIT analysis in the form of EXIT charts cannot be applied to the optimization of systematic SCLDGM codes for MIMO channels. However, in this work we explain how to design these codes using EXIT functions in a novel way that resembles DE in the sense that we test decoding convergence by tracking the evolution of messages [25]. The difference is that, while DE tracks the whole density of messages, we only track a single significant parameter, the mutual information. We have successfully applied this method to obtain good rate $1/2$ systematic SCLDGM codes for MIMO channels with a moderate number of antennas and/or bits per constellation symbol, when optimum soft-output detection, in the form of extrinsic Maximum *A Posteriori* (MAP) Log-Likelihood Ratios (LLRs) [26], is computationally feasible. Similarly to the non-systematic IRA codes in [23], the performance of our SCLDGM codes lies, in most cases, within 1 dB from the theoretical ergodic capacity limit.

Our optimized SCLDGM codes present important differences with respect to RA codes. First, the performance of regular and irregular SCLDGM codes is very similar. Second, the performance of systematic SCLDGM codes is better than that of the systematic IRA codes presented in [24] and comparable to that of the non-systematic IRA codes in [23]. Note, however, that the implementation of non-systematic IRA codes requires code doping to guarantee the convergence of the decoding algorithm. Third, unlike IRA codes, SCLDGM codes do not require an interleaver to obtain a good performance over fading channels, since an implicit interleaver is already built in the code structure.

Code design for MIMO channels is difficult for large numbers of transmitting antennas and/or high order modulations, because the complexity of optimum detection increases exponentially.

Several suboptimum detectors have been proposed, such as Soft Interference Cancellation with MMSE filtering (SIC-MMSE) [27], [28] or List Sphere Detection (LSD), to enable practical detection in these cases. Design of IRA codes employing SIC-MMSE detection is considered in [24]. In contrast, here we explain how to design SCLDGM codes considering LSD because this detector presents the best performance/complexity tradeoff in most cases. We consider the most prominent versions of LSD: Hochwald and ten Brink [7], [29], which builds the list of candidates according to the Maximum Likelihood (ML) criterion, and Vikalo *et al.* [30], which is based on the MAP criterion. EXIT analysis of MAP LSD presents an additional difficulty because the positive feedback of the *a priori* information makes the resulting EXIT function useless for code design. To overcome this limitation, we introduce an alternative detector, termed *Extrinsic* MAP LSD, that constructs two independent list sphere detections for each bit, instead of only one for each vector of symbols as in MAP LSD, and utilize its EXIT function for the analysis of MAP LSD. We have designed rate $1/2$ SCLDGM codes for both ML and MAP LSD detectors, showing their ability to approach the capacity limit. Interestingly, the code degree profiles obtained for optimum detection, ML LSD and MAP LSD are different between them.

Finally, we also study the robustness of MIMO SCLDGM codes to channel estimation errors. The impact of imperfect channel estimation on space-time decoding has been recently addressed in [31], but only focusing onto the calculation of the ML detection metrics without taking into consideration the soft information provided by the decoder. On the other hand, our approach is inspired on the Turbo principle in the sense that an initial channel estimate, obtained using a short training sequence, is subsequently refined using the soft information computed during the iterative decoding procedure [32]. Its basic premise is to formulate the ML estimate of the channel matrix taking into account both the deterministic pilot symbols and the probability density function (pdf) of the unknown information symbols. Then, this ML optimization problem is solved using the Expectation-Maximization (EM) algorithm [33]. We also explain how the LSD can be exploited to considerably reduce the complexity of the Expectation step.

The remainder of the paper is organized as follows: Section II describes Serially-Concatenated LDGM codes and their use in MIMO transmission. Section III focuses on the different LSDs considered. Code design is detailed in Section IV. Channel estimation is developed in Section V. Section VI presents simulation results for the proposed scheme with different channels and antenna configurations. Finally, Section VII is devoted to the conclusions.

II. LDGM CODES FOR MIMO CHANNELS

Systematic Low Density Generator Matrix (LDGM) codes are linear block codes with a sparse generator matrix $\mathbf{G}_{K\times N} = [\mathbf{I}_K \ \mathbf{P}_{K\times L}]$, where $\mathbf{I}_K$ denotes the $K \times K$ identity matrix. Here K/N is the code rate, $L = N - K$ is the number of parity bits in a codeword and $\mathbf{P}_{K\times L}$ is a sparse matrix. These codes are a particular case of Low Density Parity Check (LDPC) codes, since their parity check matrix $\mathbf{H}_{L\times N} = \left[\mathbf{P}^T_{L\times K} \ \mathbf{I}_L\right]$, where $(\cdot)^T$ denotes matrix transpose, is obviously also sparse. The main advantage of LDGM codes is that they have a much lower encoding complexity than general LDPC codes. However, except for high coding rates [13], LDGM codes present an error floor mainly due to their poor minimum distance. This error floor can be practically eliminated by means of a serially concatenated scheme, in which an outer LDGM code corrects the few errors remaining after the decoding of the inner LDGM code [17], [18]. We will refer to this scheme as Serially-Concatenated LDGM (SCLDGM) code.

Figure 1 plots the block diagram of a MIMO-SCLDGM coded transmitter. The input sequence $u[k] = [u_1, u_2, \ldots, u_K]$ is first encoded by a systematic LDGM outer code. Since the number of errors that have to be corrected by this code is very small, its rate $R_o = K/N_1$, $N_1 = (K + L_1)$, can be extremely high. The intermediate coded sequence $c^1[k] = [u_1, u_2, \ldots, u_K, p^1_1, p^1_2, \ldots, p^1_{L_1}]$ is then fed into the systematic inner LDGM code, which has a rate $R_i = N_1/N$, $N = N_1 + L_2$ very close to the desired global rate. The output sequence

$$c[k] = [c_1, c_2, \ldots, c_N] = [u_1, u_2, \ldots, u_K, p^1_1, p^1_2, \ldots, p^1_{L_1}, p^2_1, p^2_2, \ldots, p^2_{L_2}] \tag{1}$$

where $N = K + L_1 + L_2$, resulting from the coding stage is then directly mapped into the constellation symbols, i.e.,

$$x[k] = \mathrm{map}(c_{(k-1)M_c+1}, c_{(k-1)M_c+2}, ..., c_{kM_c}) \quad k = 1, 2, ..., N/M_c \tag{2}$$

As in [23], [24], we will restrict ourselves to Gray mapping. It must be noted that due to the nature of LDGM codes, the use of an interleaver between the coding and modulation stages is unnecessary. Finally, the resulting symbols are assigned to each antenna using a simple serial to parallel converter, that is,

$$\mathbf{x}[k] = [x[(k-1)n_t + 1], x[(k-1)n_t + 2], ..., x[kn_t]]^T \quad k = 1, 2, ..., L \tag{3}$$

where $L = N/(n_t M_c)$.

After transmission through the wireless channel, signals at reception can be written as

$$\mathbf{y}[k] = \mathbf{H}[k]\mathbf{x}[k] + \mathbf{n}[k] \quad k = 1, 2, \ldots, L \tag{4}$$

where $\mathbf{H}[k]$ is an $n_t \times n_r$ matrix that models the MIMO channel. We assume an spatially-white fast fading Rayleigh MIMO channel where the entries of $\mathbf{H}[k]$ are modeled as temporally uncorrelated, circularly-symmetric, complex-valued Gaussian random variables, i.e., $h_{ji} \sim \mathcal{CN}(0, 1)$. The components of the noise vector $\mathbf{n}[k]$ are also both spatial and temporally uncorrelated, and distributed as $\mathcal{CN}(0, N_o)$. Denoting by E_s the total energy in each transmitted vector $\mathbf{x}[k]$ and taking into account that it carries Rn_tM_c information bits, the E_b/N_0 at reception is given by $\frac{E_b}{N_0} = \frac{n_r}{Rn_tM_c}\frac{E_s}{N_0}$ where E_s/N_0 is the signal-to-noise ratio (SNR) per receiving antenna.

SCLDGM codes can be conveniently described by a factor graph [34] as shown in Fig. 2. For an SCLDGM code, each source, outer parity or inner parity bit is represented by a variable node. All variable nodes in the associated graph represent bits that are transmitted through the channnel, so they will have a message which carries the information contained in the channel observation. Check nodes represent parity constraints among the variable nodes connected to them. Outer check nodes will be denoted by f^1 while inner check nodes by f^2.

The *degree* of a node is the number of edges incident to it. A single (non-concatenated) LDGM code is *regular* if all variable nodes have the same degree, d_v. In contrast, variable nodes of an irregular LDGM code have different degrees, so an *irregular* LDGM code is characterized by its *degree profile*: the different degrees a node may have, $d_{v,i}$, $i = 1, 2, ..., D_v$, and the fraction of variable nodes having each degree, $a_{v,i}$. We consider the simplest way of assigning edges to check nodes: each check node is assigned the number of edges, d_f, resulting from dividing the total number of edges by the total number of checks. This way, check nodes have either degree d_f or d_f+1.

When specifying an SCLDGM code we have to take into account the presence of different types of variable and check nodes: variable nodes can be u_k, p_k^1 or p_k^2, while check nodes can be either f_k^1 or f_k^2. Degrees have now to be defined for each pair of node types. Let us denote by $d_{v,i}^f$, $i = 1, 2, ..., D_v^f$, the degrees of variable nodes of type v with respect to check nodes of type f. Since there is a one-to-one correspondence between check nodes and their related parity bit nodes, we therefore have only degrees $d_{u,i}^{f^1}$, $d_{u,i}^{f^2}$ and $d_{p^1,i}^{f^2}$. The number of different degrees is, respectively, $D_u^{f^1}$, $D_u^{f^2}$ and $D_{p^1}^{f^2}$. The number of edges from variable nodes of type

v to check nodes of type f is thus given by $e_v^f = \sum_{i=1}^{D_v^f} d_{v,i}^f a_{v,i}^f$. These edges are assigned to the corresponding check nodes uniformly, as in simple LDGM codes, so the degree of check nodes f with respect to variable nodes v is either d_f^v or $d_f^v + 1$. Finally, as another code parameter, let us denote by $p = L_1/(L_1+L_2)$ the fraction of outer parity bits with respect to the total number of parity bits. We will say that an SCLDGM code is *regular* when all $D_u^{f^1} = D_u^{f^2} = D_{p^1}^{f^2} = 1$. In the sequel we will drop the subindex i whenever the number of different degrees is one.

Decoding can be efficiently carried out by applying the Sum-Product Algorithm (SPA) [34] over the factor graph of the SCLDGM code. The SPA is a message-passing algorithm where messages carry statistical knowledge in the form of Log-Likelihood Ratios (LLRs) about variable nodes (bits). The SPA takes as input the channel LLR of each variable node given by

$$L_{\text{ch}} = \log \frac{P(\mathbf{y}|c_k = 1)}{P(\mathbf{y}|c_k = 0)} = \log \frac{P(c_k = 1|\mathbf{y})}{P(c_k = 0|\mathbf{y})} - \underbrace{\log \frac{P(c_k = 1)}{P(c_k = 0)}}_{L_k} \tag{5}$$

There are two types of messages in the SPA: variable-to-check, given by the *sum* of all incoming messages except that coming from the target check node

$$L_{v\to c} = \sum_{c' \neq c} L_{c'\to v} + L_{\text{ch}} \tag{6}$$

and check-to-variable, given by the *product* (in the $\tanh(\cdot/2)$ domain) of all incoming messages except that coming from the target variable node

$$\tanh \frac{L_{c\to v}}{2} = \prod_{v' \neq v} \tanh \frac{L_{v'\to c}}{2} \tag{7}$$

After an enough number of iterations has been performed, a decision is made using the *a posteriori* LLR of source bits

$$L_u = \sum_{c} L_{c\to v} + L_{\text{ch}} \tag{8}$$

The channel LLR given by Eq. 5 can be exactly computed by the optimum *A Posteriori* Probability (APP) MIMO detector as (to simplify notation, we eliminate index $[k]$)

$$L_{\text{ch}} = \log \frac{\displaystyle\sum_{\mathbf{x}\in X_k^+} \exp\left(-\frac{1}{N_0}\|\mathbf{y} - \mathbf{H}\mathbf{x}\|^2 + \sum_{i=1}^{n_t M_c} x_i \frac{L_i}{2}\right)}{\displaystyle\sum_{\mathbf{x}\in X_k^-} \exp\left(-\frac{1}{N_0}\|\mathbf{y} - \mathbf{H}\mathbf{x}\|^2 + \sum_{i=1}^{n_t M_c} x_i \frac{L_i}{2}\right)} - L_k \tag{9}$$

where X_k^+ and X_k^- represent the set of all transmitted symbol vectors $\mathbf{x}$ when bit $c_k = 1$ and $c_k = 0$, respectively. Also, x_i is $+1$ if bit $c_i = 1$ and -1 if bit $c_i = 0$. However, the complexity of APP detection grows exponentially in both the number of transmitting antennas and constellation size, being infeasible in many cases of practical interest. To overcome this limitation, the sum in Eq. 9 over $\mathbf{x} \in X_k^+$ (resp. $\mathbf{x} \in X_k^-$) can be computed using only the most relevant terms. In the next Section, we detail how such a list of terms can be efficiently constructed.

III. List Sphere detection

The idea of List Sphere Detection (LSD) is to approximately calculate Eq. (9), whose terms in the summations are in fact, except for an additive constant α, the logarithm of the APP of a transmitted vector $\mathbf{x}$

$$\log P(\mathbf{x}|\mathbf{y}) = -\frac{1}{N_0}\|\mathbf{y} - \mathbf{H}\mathbf{x}\|^2 + \sum_{i=1}^{n_t M_c} x_i \frac{L_i}{2} + \alpha, \tag{10}$$

using a list of just N_{cand} candidate vectors $\mathbf{x}$.

The Maximum Likelihood List Sphere Detector (ML LSD) proposed by Hochwald and ten Brink [7] constructs the list using the N_{cand} most likely (ML) vectors. That is, those that maximize just the first term in Eq. (10)

$$\log P(\mathbf{y}|\mathbf{x}) = -\frac{1}{N_0}\|\mathbf{y} - \mathbf{H}\mathbf{x}\|^2 + \alpha' \tag{11}$$

The list is constructed using a modified version of the Sphere Detector (SD) [35], [36], which efficiently finds the constellation points inside a hypersphere centered on the unconstrained ML estimate of the transmitted vector.

As we will see in Section VI, the performance of the decoding process depends on the size of the candidate list (N_{cand}). When N_{cand} is high we will have to compute more likelihoods, and more processing will be needed in detector, but the performance will be better. However, the performance degrades when using low values of N_{cand} due to the smaller amount of information processed by the algorithm. Therefore, there is a tradeoff between efficiency and performance in the choice of N_{cand}. Keeping the number of candidates of the sphere detector constant while increasing the number of antennas leads to a linear increase in complexity.

An alternative approach, termed as MAP LSD and proposed by Vikalo *et al.* [30], consists in building the list of the N_{cand} vectors with highest APP, according to Eq. 10. This way we are

actually finding the most significant terms for the summations involved in the computation of the channel LLR. However, when used in an iterative receiver this method has to perform the complete tree search each time new *a priori* bit probabilities are available from other receiver stages. On the other hand, the complexity of ML LSD is smaller, since in this case the search for the most likely vectors is performed only once and the corresponding likelihoods stored for their use in successive iterations.

Notice, however, that in both approaches a candidate in the list is a vector of symbols and no consideration is made about the value of each bit in the candidate, as required in Eq. (9). Considering only one candidate list results in the chance of having no candidates for computing one of the sums in Eq. (9). As suggested in [7], this can be solved by assigning a minimum value (instead of zero) to the sum and by applying a threshold lower than that used in the SPA decoder to the obtained LLRs [7], which leads to additional information loss. Building only one candidate list gives rise to another problem, positive feedback, in MAP LSD. Although the *a priori* LLR of the bit being processed, L_k, is substracted in Eq. (9) to obtain the extrinsic channel LLR, it is implicitly considered in the construction of the candidate list. Note that a high *a priori* LLR of the bit being considered leads to the inclusion in the list of those candidates for which that bit has the value suggested by the *a priori* bit LLR. This effect is more pronounced as the size of the candidate list gets smaller and, clearly, is not compensated by just substracting the *a priori* LLR. This positive feedback is clearly shown by the fact that the mutual information of the output LLRs produced by the MAP LSD (see Fig. 3) is higher than that of the optimum APP detector, which indicates that additional information is contained in these output LLRs. Indeed, this mutual information does not constitute a *true* EXIT chart because it does not only measure extrinsic information but also *a priori* information. Since it is only the extrinsic information transfer what determines decoding convergence, it would be necessary to cancel the contribution of the *a priori* information from the output LLRs when computing the actual EXIT chart of this detector. However, this cannot be done because *a priori* information is implicitely introduced by the particular way the candidate list is built. To overcome this limitation, we consider what we

call *Extrinsic* LSD, which consists in rewriting Eq. (9) as

$$L_{\text{ch}} = \log \frac{\sum_{\mathbf{x}\in X_k^+} \exp\left(-\frac{1}{N_0}\|\mathbf{y}-\mathbf{H}\mathbf{x}\|^2 + \sum_{i=1,i\neq k}^{n_t M_c} x_i \frac{L_i}{2}\right)}{\sum_{\mathbf{x}\in X_k^-} \exp\left(-\frac{1}{N_0}\|\mathbf{y}-\mathbf{H}\mathbf{x}\|^2 + \sum_{i=1,i\neq k}^{n_t M_c} x_i \frac{L_i}{2}\right)} \tag{12}$$

Then, separate lists for the numerator and the denominator and for each bit in a symbol vector are constructed. This means $2n_tM_c$ candidate lists for computing the bit channel LLRs in a symbol vector, instead of only one as in MAP LSD. The complexity of this approach is $2n_tM_c$ times higher that that of MAP LSD, but its expected performance is better, especially when the number of candidates is low. In addition, since it does not suffer from positive feedback, its *true* EXIT function can be computed, enabling code design. However, note that if MAP LSD is used with a high number of candidates, the effect of the *a priori* LLR of the bit under consideration in the obtained list is less severe. This motivates us to use MAP LSD in the final implementation shown in Section VI, even though code design is performed using the EXIT function of the Extrinsic LSD.

IV. Code design

Predicting the convergence of the coding scheme can be carried out by tracking the densities of the different types of messages involved in the SPA. This constitutes the Density Evolution (DE) approach [22]. If no particular density is assumed for the messages, densities have to be described by quantizing the probability space and performing complex operations to obtain the density of an output message from the densities of the incoming messages. In order to reduce computational complexity, message densities can be assumed to be symmetric Gaussian, and thus only the mean has to be tracked [37]. An alternative approach is to track a significant parameter associated to the message density, where significance has to be understood in terms of predicting convergence threshold. In this sense, mutual information between the message density and the *a priori* bit density has been revealed to be significant. Since messages represent extrinsic information about bits, their related mutual information has been termed as EXtrinsic Information Transfer functions [38]. Let us denote by $I_M \equiv I(M;V) = 1 - H(V|M)$ the mutual information between the variable-to-check message $M \equiv V \rightarrow C$ and the *a priori* density of bit V. Mutual information for a check-to-variable message is defined in the same way. As a

message $M \equiv V \rightarrow C$ is characterized by I_M, the incoming messages $M'_l \equiv C_l \rightarrow V$ are also characterized by their mutual information, $I_{M'_l}$. The task is then to express the mutual information of an output message as a function of the mutual informations of incoming messages.

Mutual information for a message produced by a variable node can be computed just taking into account that incoming messages play the same role as the channel LLR in Eq. 6. A reasonable assumption is to consider each incoming message M as the output LLR of an independent BIAWGN channel with noise variance σ^2. Note that for a BIAWGN channel the output LLR $L_{\rm ch}$ conditioned on the transmitted bit $x_k = \pm 1$ is (symmetric) Gaussian with mean $\pm 2/\sigma^2$ and variance $4/\sigma^2$. This is what DE does when the symmetric Gaussian assumption is used, but now the density parameter which is tracked, mutual information instead of the mean, is more related with code convergence. The mutual information of the output LLR of a BIAWGN channel with respect to the *a priori* bit density is given by [10]

$$J(\sigma^2) \equiv I(M;V) = \mathbb{E}_{M,V}\left[\log_2 \frac{f(v,m)}{f(v)f(m)}\right] = 1 - \mathbb{E}_M\left[\log_2(1+e^{-m})\right] \tag{13}$$

where $\mathbb{E}_Z$ denotes the expectation operator with respect to the random variable Z. Notice that this mutual information depends only on the channel variance[1] σ^2. Therefore, $J^{-1}(I)$ gives the channel variance corresponding to an incoming message with mutual information I. As shown in [39], there is a one-to-one correspondence between mutual information, I, and channel variance, σ^2. As a consequence, tracking mutual information is equivalent to tracking the mean. However, the difference between our approach and DE with Gaussian approximation resides in the way the value for the tracked parameter is related to its value in the previous iteration.

The mutual information of SPA variable-to-check messages is thus given by

$$I_v = J\left(\sum_m J^{-1}(I_m)\right) \tag{14}$$

where I_m is the mutual information of the incoming message m.

In order to compute the mutual information of a check-to-variable message, it is convenient to resort to a duality property of the Binary Erasure Channel (BEC) that is very accurate (although not exact) for the BIAWGN channel [10]. This property relates the mutual information of the

[1]In [10] the argument of the J function is the channel standard deviation, σ. We prefer to use σ^2 because it leads to more compact expressions.

length-d_f single-parity check (SPC) code to that of the length-d_f repetition (REP) code by

$$I_{\mathrm{SPC}}(I_m, d_f) \approx 1-I_{\mathrm{REP}}(1-I_m, d_f) = 1-J\big((d_f-1)J^{-1}(1-I_m)\big) \tag{15}$$

Using Eqs. (14)-(15) for the factor graph of a regular SCLDGM code we have

$$I_u^{f^1} = J\left((d_u^{f^1}-1)J^{-1}(I_{f^1}^u)+d_u^{f^2}J^{-1}(I_{f^2}^u)+J^{-1}(I_{\mathrm{det}}^u)\right) \tag{16}$$

$$I_u^{f^2} = J\left(d_u^{f^1}J^{-1}(I_{f^1}^u)+(d_u^{f^2}-1)J^{-1}(I_{f^2}^u)+J^{-1}(I_{\mathrm{det}}^u)\right) \tag{17}$$

$$I_{p^1}^{f^1} = J\left(d_{p^1}^{f^2}J^{-1}(I_{f^2}^{p^1})+J^{-1}(I_{\mathrm{det}}^{p^1})\right) \tag{18}$$

$$I_{p^1}^{f^2} = J\left((d_{p^1}^{f^2}-1)J^{-1}(I_{f^2}^{p^1})+J^{-1}(I_{f^1}^{p^1})+J^{-1}(I_{\mathrm{det}}^{p^1})\right) \tag{19}$$

$$I_{p^2}^{f^2} = J\left(J^{-1}(I_{\mathrm{det}}^{p^2})\right) = I_{\mathrm{det}}^{p^2} \tag{20}$$

$$I_{f^1}^u = 1-J\Big((d_{f^1}-1)J^{-1}(1-I_u^{f^1})+J^{-1}(1-I_{p^1}^{f^1})\Big) \tag{21}$$

$$I_{f^1}^{p^1} = 1-J\Big(d_{f^1}J^{-1}(1-I_u^{f^1})\Big) \tag{22}$$

For messages from inner checks to outer variable nodes, we have to distinguish between two types of inner check nodes: those that are connected to outer parity bits (for simplicity, we assume in our designs that an inner check may receive at most one edge from the outer parity bits) and those which are not. We denote them, respectively, f^2, a and f^2, b.

$$I_{f^2,a}^u = 1-J\left(J^{-1}(1-I_{p^1}^{f^2})+(d_{f^2}-2)J^{-1}(1-I_u^{f^2})+J^{-1}(1-I_{p^2}^{f^2})\right) \tag{23}$$

$$I_{f^2,b}^u = 1-J\left((d_{f^2}-1)J^{-1}(1-I_u^{f^2})+J^{-1}(1-I_{p^2}^{f^2})\right) \tag{24}$$

Messages $f^2 \to u$ will then have an associated mutual information given by the sum of $I_{f^2,a}^u$ and $I_{f^2,b}^u$, weighted by the fraction of edges carrying each type of messages. Denoting by $a = L_1 d_{p^1}^{f^2}$ the number of inner checks that are connected to outer parity bits, this results in

$$I_{f^2}^u = \frac{a(d_{f^2}-1)I_{f^2,a}^u + (L_2-a)d_{f^2}I_{f^2,b}^u}{a(d_{f^2}-1)+(L_2-a)d_{f^2}} \tag{25}$$

Extension of the previous equations to irregular SCLDGM codes is quite straighforward, just by considering that the mutual information associated to a given type of messages is the mean, weighted by the correspondig fraction of edges, of the mutual information of messages originating at nodes having a certain degree. However, as we will show in Section VI irregular codes do not present a substantial improvement in performance.

Code convergence is tested by simulating the evolution of the SPA. For a fixed E_b/N_0 we start with all I's equal to zero and then we iteratively compute their values. This is exactly what the SPA does but we now use representatives of messages (their associated I's) instead of their actual values. We say that the code converges when we find a sequence of I's that finally leads to $I_u = 1$, where I_u is the mutual information associated to the *a posteriori* LLRs of bits u (see Eq. 8). When I_u is almost equal to, but strictly less than 1, convergence is achieved but with a significant error-floor.

Let us first focus on the messages produced by the MIMO detector. Since output LLRs (see Eq. 9) are the result of a complex operation, it is convenient to obtain the actual mutual information of output messages via Monte Carlo simulation. For a fixed E_s/N_0, we simulate the transmission through a MIMO channel and then we fix the mutual information of *a priori* messages to a certain value, I_v. Afterwards, we generate *a priori* messages considering them as the output LLR of a BIAWGN channel with variance $J^{-1}(I_v)$, and feed them to the MIMO detector. Then, the mutual information of messages produced by the MIMO detector is measured. As an example, Figure 3 plots the EXIT chart for the ML LSD and the Extrinsic LSD MIMO detectors, as well as the mutual information of the output LLRs produced by the MAP LSD (which is not a *true* EXIT chart due to positive feedback), for 4×4 QPSK at $E_s/N_0 = 2$ dB and different sizes of the candidate list. Fig. 3 also depicts the EXIT chart of the optimum detector, in which case the number of processed vectors is 256. It is apparent from Fig. 3 that EXIT functions of a MIMO detector, $I_d(I_v, E_s/N_0)$, are well approximated just by third-order polynomials. This provides us with a quick means of evaluating the EXIT function of the MIMO detector for a given E_s/N_0 and I_v. We have also observed that better performance is achieved when the three types of bits (source, outer parity and inner parity) are not mixed to form a symbol vector, i.e., bits forming a vector of symbols are of the same type. When tracing the SPA with mutual information of messages, the detector is independently applied to each type of bits, so we have to separately consider messages from the detector to each of the variable node types, i.e., $I^u_{\rm det}$, $I^{p^1}_{\rm det}$, $I^{p^2}_{\rm det}$.

The previous discussion suggests a straightforward way to search for the best codes. We start considering an initial channel E_b/N_0. For this value, we simulate the SPA evolution for all possible code degree profiles and we discard those for which the SPA does not converge. Next, if we lower the E_b/N_0 value and repeat the same simulation we will find out that some of the remaining codes still converge while the others that do not converge are now discarded. We

proceed in the same way, lowering the E_b/N_0 value until only one convergent code remains. This code is the optimum and the E_b/N_0 value is its convergence threshold. As an example, Fig 4 (left) shows the messages' mutual information evolution through decoding iterations for a good SCLDGM code in a 4×4 QPSK channel when $E_b/N_0 = 1.75$ dB. Note that mutual information of outer variable-to-outer check messages, "$u - f^1$", which is roughly the same of that corresponding to the L_u messages used for making the final decision (see Eq. (8)), does not reach $I_u^{f^1} = 1$, so we are still in the non-convergence region. The outer code gives no help to the convergence because mutual information of outer check-to-outer variable messages ("$f^1 - u$") remains always equal to zero until the 85th iteration. On the other hand, Fig. 4 (right) shows the decoding behaviour when $E_b/N_0 = 1.8$ dB. Now the outer code starts to help from iteration 65, leading to overall convergence from iteration 85: mutual information of "$u - f^1$" messages is there very close to one. From this EXIT trajectories, we can conclude that the convergence threshold is $E_b/N_0 = 1.8$ dB. An error-floor still is present, but it is low enough (as we will see in the following section) and cannot be observed by inspection of the EXIT function.

We applied the previous procedure for the design of good rate $1/2$ regular SCLDGM codes for different antenna configurations, modulation formats and detectors. We carried out an exhaustive search, varying the code parameters between the following limits: $0.01 \leq p \leq 0.05$, with increments of 0.005; $3 \leq d_u^{f^1} \leq 5$; $2 \leq d_u^{f^2} \leq 30$; and $2 \leq d_{p^1}^{f^2} \leq 30$, fixing also the maximum value for d_{f^2} to 10. The obtained codes are presented in Table I, together with their convergence threshold predicted by EXIT analysis. Note the extraordinary performance of the resulting codes, since the gap to the constrained-input ergodic capacity limit is less than 1 dB in almost all cases. This performance is similar to that of the non-systematic IRA codes in [23] and better than that of the systematic IRA codes in [24].

V. Channel estimation

Soft information calculated during the decoding procedure can be efficiently exploited to improve channel estimation by combining LSD with the Expectation Maximization (EM) algorithm [33]. We consider ML estimation of the channel matrix assuming that data streams contain deterministic pilot symbols and random information symbols whose pdf is known. The resulting optimization problem can be numerically solved with the EM algorithm, whose complexity will be substantially reduced by taking advantage of the LSD.

Let us start by considering the ML estimation of a MIMO channel given by

$$\hat{\mathbf{H}} = \arg\max_{\mathbf{H}} f_{\tilde{\mathbf{y}}|\mathbf{H}}(\tilde{\mathbf{y}}), \tag{26}$$

where $f_{\tilde{\mathbf{y}}|\mathbf{H}}(\tilde{\mathbf{y}})$ is the pdf of all the observations $\tilde{\mathbf{y}} = [\mathbf{y}^T[0]\ \mathbf{y}^T[1]\ \cdots\ \mathbf{y}^T[B]]^T$, which depends on the channel matrix $\mathbf{H}$ to be estimated. We will assume that the channel remains constant during B time slots (i.e., block fading). In general, B will be different from L.

Next, let us define the set of "complete data", necessary when stating the EM algorithm, as $\tilde{\mathbf{y}}_c = [\mathbf{y}_c^T[1]\ \mathbf{y}_c^T[2]\ \cdots\ \mathbf{y}_c^T[B]]^T$ where $\mathbf{y}_c[k] = [\mathbf{x}[k]^T\ \mathbf{y}[k]^T]^T$. The EM algorithm relies on the computation of the channel estimation in each step as

$$\hat{\mathbf{H}}_{i+1} = \arg\max_{\mathbf{H}} \mathbb{E}_{\tilde{\mathbf{y}}_c|\tilde{\mathbf{y}},\hat{\mathbf{H}}_i} \log(f_{\tilde{\mathbf{y}}_c|\mathbf{H}}(\tilde{\mathbf{y}}_c)), \tag{27}$$

Elaborating (27) we have

$$\begin{aligned}
\hat{\mathbf{H}}_{i+1} &= \arg\max_{\mathbf{H}} \mathbb{E}_{\tilde{\mathbf{x}}|\tilde{\mathbf{y}},\hat{\mathbf{H}}_i} \log(f_{\tilde{\mathbf{y}}|\tilde{\mathbf{x}}}(\tilde{\mathbf{y}}) \cdot f_{\tilde{\mathbf{x}}}(\tilde{\mathbf{x}})) = \arg\max_{\mathbf{H}} \mathbb{E}_{\tilde{\mathbf{x}}|\tilde{\mathbf{y}},\hat{\mathbf{H}}_i} \log(f_{\tilde{\mathbf{y}}|\tilde{\mathbf{x}}}(\tilde{\mathbf{y}})) \\
&= \arg\max_{\mathbf{H}} \mathbb{E}_{\tilde{\mathbf{x}}|\tilde{\mathbf{y}},\hat{\mathbf{H}}_i} \sum_{k=1}^{B} \|\mathbf{y}[k] - \mathbf{H}\mathbf{x}[k]\|^2 = \arg\max_{\mathbf{H}} \sum_{k=1}^{B} \mathbb{E}_{\mathbf{x}[k]|\tilde{\mathbf{y}},\hat{\mathbf{H}}_i} \|\mathbf{y}[k] - \mathbf{H}\mathbf{x}[k]\|^2 \\
&= \arg\max_{\mathbf{H}} \sum_{k=1}^{B} \mathbb{E}_{\mathbf{x}[k]|\mathbf{y}[k],\hat{\mathbf{H}}_i} \|\mathbf{y}[k] - \mathbf{H}\mathbf{x}[k]\|^2
\end{aligned} \tag{28}$$

which is a quadratic expresion with respect to $\mathbf{H}$ with the following closed-form solution

$$\hat{\mathbf{H}}_{i+1} = \left(\sum_{k=1}^{B} \mathbb{E}_{\mathbf{x}[k]|\mathbf{y}[k],\hat{\mathbf{H}}_i} \mathbf{R}_{yx}[k] \right) \times \left(\sum_{k=1}^{B} \mathbb{E}_{\mathbf{x}[k]|\mathbf{y}[k],\hat{\mathbf{H}}_i} \mathbf{R}_{x}[k] \right)^{-1} \tag{29}$$

where $\mathbf{R}_{yx}[k] = \mathbf{y}[k]\mathbf{x}^H[k]$ and $\mathbf{R}_x[k] = \mathbf{x}[k]\mathbf{x}^H[k]$.

If we consider that the first P transmitted symbols correspond to a known pilot sequence, the channel estimator simplifies to

$$\hat{\mathbf{H}}_{i+1} = \left(\sum_{k=1}^{P} \mathbf{R}_{yx}[k] + \sum_{k=P+1}^{B} \mathbb{E}_{\mathbf{x}[k]|\mathbf{y}[k],\hat{\mathbf{H}}_i} \mathbf{R}_{yx}[k] \right) \times \left(\sum_{k=1}^{P} \mathbf{R}_{x}[k] + \sum_{k=P+1}^{B} \mathbb{E}_{\mathbf{x}[k]|\mathbf{y}[k],\hat{\mathbf{H}}_i} \mathbf{R}_{x}[k] \right)^{-1} \tag{30}$$

It is interesting to note that (30) can be viewed as a generalized Least-Squares (LS) channel estimator where for the unknown symbols the correlations $\mathbf{R}_{yx}[k]$ and $\mathbf{R}_x[k]$ are obtained by averaging with respect to the *a posteriori* pdf $P(\mathbf{x}|\mathbf{y}, \hat{\mathbf{H}}_i)$ of those symbols. The lower the variance associated to this pdf, the more information we have about the unknown symbols and,

thus, the much more they look like pilot symbols regarding estimation. In this way, the length of the pilot sequence, P, can be reduced with respect to pure LS channel estimation.

The main problem when estimating the channel via the EM algorithm is similar to that in the APP detector: complexity of the expectation calculation in (30) is exponential in the number of antennas and constellation size. The LSD alleviates this problem: by combining the sphere detection and the EM algorithms, the average in (30) is not calculated over all possible transmitted vectors, but only over the candidate list obtained by the LSD, i.e.,

$$\mathbb{E}_{\mathbf{x}[k]|\mathbf{y}[k],\hat{\mathbf{H}}_i}\mathbf{R}_x[k] = \sum_{\mathbf{x}[k]\in\mathcal{X}} \mathbf{R}_x[k]P(\mathbf{x}[k]|\mathbf{y}[k],\hat{\mathbf{H}}_i) \approx \sum_{\mathbf{x}[k]\in\mathcal{L}} \mathbf{R}_x[k]P(\mathbf{x}[k]|\mathbf{y}[k],\hat{\mathbf{H}}_i) \tag{31}$$

where $\mathcal{X}$ is the set of all possible transmitted symbols, with $|\mathcal{X}| = 2^{n_t M_c}$, whereas $\mathcal{L} = \{\mathbf{x}_1, \mathbf{x}_2, ..., \mathbf{x}_{N_{\text{cand}}}\}$ denotes the candidate list obtained by the LSD. The same approximation can be made for computing $\mathbb{E}_{\mathbf{x}[k]|\mathbf{y}[k],\hat{\mathbf{H}}_i}\mathbf{R}_{yx}[k]$. Moreover, the MAP LSD already computes the APPs $P(\mathbf{x}[k]|\mathbf{y}[k])$ needed for the expectation.

VI. Simulation Results

Computer simulations were carried out to evaluate the performance of the obtained SCLDGM codes in practical cases where blocks of finite length are transmitted. In the first simulation experiments we assumed that the MIMO channel changes randomly and independently from one symbol vector to another (fast fading ergodic channel) and is known at the receiver.

Fig. 5 compares the performance of regular and irregular SCLDGM codes for 4×4, QPSK and optimum detection. The optimized irregular SCLDGM code is given by

$$p = 3\% \quad d_u^{f^1} = 3 \quad d_u^{f^2} = \{4, 5, 21\} \quad a_u^{f^2} = \{0.5, 0.4, 0.1\} \quad d_{p^1}^{f^2} = 10 \tag{32}$$

whereas the regular code is that of Table I. Their theoretical thresholds are 1.75 dB and 1.80 dB, respectively. Two block sizes are considered: $N = 20000$ and $N = 100000$ coded bits. Notice that practical convergence thresholds are higher than those predicted by EXIT function analysis. This is because EXIT analysis assumes infinite-length data blocks. Indeed, notice that the higher the block length is, the closer the convergence threshold is to the theoretical value calculated with the EXIT functions. Fig. 5 also shows that the difference in performance between regular and irregular codes is very small (around 0.05 dB). For this reason only regular SCLDGM codes are considered in the paper, since this greatly reduces the search space and the code regularity usually allows easier hardware implementation.

Code performance for asymmetric antenna configurations (4×1 and 4×2 QPSK) and $N = 100000$ coded bits is shown in Fig. 6. In this case, the detector EXIT function has a positive slope, and it is very different from that of a SISO channel (which is an almost horizontal straight line). This means that code design is important to properly match the detector EXIT function. Indeed, notice the difference in performance between an SCLDGM code optimized for the SISO case (see Table I) but applied over the MIMO channel and an SCLDGM code specifically designed for the antenna configuration and modulation format under consideration. For instance, for 4×2 QPSK and a BER$= 10^{-4}$, the performance difference is around 1.3 dB. This gap is much larger (around 5 dB) for the 4×1 system. This is explained by the fact that, for the same number of transmitting antennas, using less receiving antennas makes the detector EXIT function steeper [10] and, thus, it is critical that the code matches it (and not the horizontal like characteristic of SISO channels). Notice that the convergence thresholds obtained through simulation practically overlap with the theoretical ones presented in Table I, and they are very close to the constrained capacities (gap of 0.8 dB and 1.8 dB for the 4×2 and 4×1 systems, respectively).

The effect of code and detector mismatch is shown in Fig. 7 for a 4×4 16-QAM system and a block of $N = 20000$ coded bits (which will be the length used in the sequel). First notice the performance difference between a code optimized for the used detector and a code optimized for a different detector: for a target BER of 10^{-4}, employing MAP LSD with 32 candidates and its optimized code requires an $E_b/N_0 = 5.9$ dB, while using the same detector but with a code optimized for ML LSD with 128 candidates needs an $E_b/N_0 = 6.45$ dB. If ML LSD with 128 candidates is considered, using its optimized code requires an $E_b/N_0 = 6.25$ dB, while using a code optimized for MAP LSD with 32 candidates needs an $E_b/N_0 = 6.5$ dB. In this latter case, the effect of code and detector mismatch is less severe than in the former.

We next focus on comparing the performance of LSD with respect to that of optimum MAP detection when the optimized codes for each respective detector are utilized. Fig. 8 shows the performance curves for 2×2 antennas using 16-QAM. Optimum detection needs to process $2^{n_t M_c} = 2^8 = 256$ possible symbol vectors. See how using ML LSD with half of the total number of candidates (128) renders near optimum performance, while decreasing the number of candidates to one quarter of the total (64) results in little performance degradation. Also note that MAP LSD needs only $1/8$ of the total number of candidates (32) to provide near optimum optimum performance (instead of the 128 candidates required by ML LSD). The convergence

threshold obtained through simulations is very close to the theoretical one in Table I, and only 1.0 dB away from the constrained capacity.

Optimum MAP detection is not feasible when considering 2×2 64-QAM, since the total number of possible vector symbols is $2^{n_t M_c} = 2^{12} = 4096$. However, very good performance is obtained with suboptimum LSD, as shown in Fig. 9. For a target BER of 10^{-5}, the best performance is achieved by MAP LSD with 128 candidates, which requires an $E_b/N_0 = 7.9$ dB, only 0.3 dB from the theoretical threshold of Table I and 1.25 dB away from the constrained-input ergodic capacity. Halving the number of candidates (32) results in 0.4 dB degradation. Note how eight times the number of candidates (256) is needed to obtain similar performance if ML LSD is used.

Similar conclusions can be drawn from Fig. 10 for 4×4 16-QAM. The total number of candidates in this case is 65536. The best performance is obtained by MAP LSD with 256 candidates ($1/256$ of the total), requiring an $E_b/N_0 = 5.15$ dB for a target BER of 10^{-5}, which is 0.35 dB away from the theoretical threshold in Table I and only 1.05 dB away from the constrained-input ergodic capacity. Very little performance degradation (0.1 dB) results from considering half (128) of such number of candidates. However, further reducing the size of the candidate list to 64 and 32 increases the required E_b/N_0 up to 5.7 dB and 6.1 dB, respectively. See how 512 candidates are needed by ML LSD to obtain a performance similar to that of MAP LSD with 64 candidates. Using ML LSD with less candidates results in more performance degradation.

Notice that for small numbers of candidates (with respect to the total number of possible vectors), the gaps between the theoretical thresholds and those observed in the simulations increase. This can be explained realizing that in this case the pdf of the output LLRs of ML/MAP LSD is far different from the Gaussian one assumed in our optimization procedure. Using a low number of candidates results in many LLRs taking extreme values because the list contains much more candidates for the numerator than for the denominator (or *vice versa*). LLR values greater than 8 (less than -8) are truncated to $+8$ (-8), producing a pdf with high peaks in these two values.

Finally, we carried out a simulation experiment to illustrate the performance when the channel is estimated according to the procedure explained in Section V. We considered a sequence of $N = 20000$ coded bits transmitted over a 4×4 MIMO channel using 16-QAM. This corresponds

to the transmission of $L = 1250$ vectors of symbols. The transmitted bits are splitted into 10 blocks of $B{-}P{=}125$ information vector symbols, and then P pilot vector symbols are appended to each block. Block fading is assumed: the channel remains constant during the transmission of each block of B symbols and randomly changes from one block to another. In the training period we transmit the 16-QAM symbols with highest energy using only one antenna at each time slot, switching the selected transmit antenna between consecutive time slots to guarantee orthogonality of the training sequence. In Fig. 11, the E_b/N_0 has been properly normalized to account for the energy "wasted" in pilot symbols. We have also assumed that only one iteration in the EM algorithm is performed for each detection iteration. Fig. 11 shows the BER curves for $P{=}4$, 8 and 12. It can be seen that with a small number of pilot symbols such as 8 (6.01% of the frame size) and 12 (8.75%) and with the MAP LSD with 64 candidates, the performance degradation due to imperfect channel estimation is less than 1 dB. Larger degradation is obtained if a lower number of pilot symbols are used and/or ML LSD (even with 256 candidates) is employed. Notice from Fig. 11 that when the channel is perfectly known, there is a diffrerence in performance with respect to the pure ergodic case of about 1 dB. This is because in this computer experiment the channel is not purely ergodic but block fading. Obviously, the performance tends to the case of fast fading if the codeword length is increased and B is kept fixed.

VII. Conclusions

We have shown the ability of Serially-Concatenated LDGM (SCLDGM) codes to approach the ergodic capacity of MIMO channels. Using List Sphere Detection (LSD) we show how complexity can be kept at a low level when the number of antennas and modulation levels increase. Both Maximum Likelihood (ML) and Maximum *A Posteriori* (MAP) LSDs have been considered. We have explained how to use EXIT functions to design SCLDGM codes for MIMO channels. Our design procedure takes into account not only the number of antennas and the modulation format but also the particular detector employed: optimum MAP, ML LSD or MAP LSD. Computer simulations illustrate how the proposed design procedure accurately predicts the code convergence threshold. The optimized codes show a remarkable ability to approach the channel capacity limits and clearly outperform existing IRA codes and LDPC codes with low encoding complexity. Finally, we have also shown how the performance is not severely degraded when the channel is imperfectly estimated.

REFERENCES

[1] C. Berrou, A. Glavieux, and P. Thitimajshima, "Near Shannon limit error-correcting coding and decoding: Turbo-codes," in *ICC '93*, Geneva, Switzerland, May 1993, pp. 1064–1070.

[2] R. G. Gallager, *Low Density Parity Check Codes*. Research Monograph 21. MIT Press, Cambridge, Mass., 1963.

[3] D. MacKay, "Good error-correcting codes based on very sparse matrices," *IEEE Trans. Inform. Theory*, vol. 45, no. 2, pp. 399–431, 1999.

[4] S. Y. Chung, D. Forney, T. J. Richardson, and R. Urbanke, "On the design of Low-Density Parity-Check codes within 0.0045 dB of the Shannon limit," *IEEE Commun. Lett.*, vol. 5, no. 2, pp. 58–60, Feb. 2001.

[5] R. Narayanaswami, "Coded modulation with Low Density Parity Check codes," Master's thesis, Texas A&M University, College Station, TX, June 2001. [Online]. Available: http://ee.tamu.edu/ krishna/PAPERS/ravithesis.ps

[6] J. Hou, P. H. Siegel, L. B. Milstein, and H. D. Pfister, "Capacity-approaching bandwidth-efficient coded modulation schemes based on Low-Density Parity-Check codes," *IEEE Trans. Inform. Theory*, vol. 49, no. 9, pp. 2141–2155, Sept. 2003.

[7] B. M. Hochwald and S. ten Brink, "Achieving near-capacity on a multiple-antenna channel," *IEEE Trans. Commun.*, vol. 51, no. 3, pp. 389–399, Mar. 2003.

[8] B. Lu, X. Wang, and K. R. Narayanan, "LDPC-based space-time coded OFDM systems over correlated fading channels," *IEEE Trans. Commun.*, vol. 50, no. 1, pp. 74–88, Jan. 2003.

[9] B. Lu, G. Yue, and X. Wang, "Performance analysis and design optimization of LDPC-coded MIMO OFDM systems," *IEEE Trans. Signal Processing*, vol. 52, no. 2, pp. 348–361, Feb. 2004.

[10] S. ten Brink, G. Kramer, and A. Ashikhmin, "Design of Low-Density Parity-Check codes for modulation and detection," *IEEE Trans. Commun.*, vol. 52, no. 4, pp. 670–678, Apr. 2004.

[11] J. Hou, P. H. Siegel, and L. B. Milstein, "Design of Multi-Input Multi-Output systems based on Low-Density Parity-Check codes," *IEEE Trans. Inform. Theory*, vol. 53, no. 4, pp. 601–611, Apr. 2005.

[12] H. Zhong and T. Zhang, "Block-LDPC: a practical LDPC coding system design approach," *IEEE Trans. Circuits Syst. I*, vol. 52, no. 4, pp. 766–775, Apr. 2005.

[13] J. F. Cheng and R. J. McEliece, "Some high-rate near capacity codecs for the Gaussian channel," in *Proc.* 34^{th} *Allerton Conf. on Communications, Control and Computing*, Oct. 1996.

[14] D. Divsalar, H. Jin, and R. J. McEliece, "Coding theorems for 'turbo-like' codes," in *Proc. of 36th Allerton Conf. on Communication, Control, and Computing*, Allerton, Illinois, Sept. 1998, pp. 201–210.

[15] *IEEE 802 Part 16: Air Interface for Fixed and Mobile Broadband Wireless Access Systems*, IEEE Computer Society and the IEEE Microwave Theory and Techniques Society Std., Feb. 2006.

[16] "HT PHY specification," Enhanced Wireless Consortium (EWC), Dec. 2005, v1.27. [Online]. Available: www.enhancedwirelessconsortium.org

[17] J. Garcia-Frias and W. Zhong, "Approaching Shannon performance by iterative decoding of linear codes with low-density generator matrix," *IEEE Commun. Lett.*, vol. 7, no. 6, pp. 266–268, June 2003.

[18] W. Zhong and J. Garcia-Frias, "LDGM codes for channel coding and joint source-channel coding of correlated sources," *EURASIP Journal on Applied Signal Processing*, vol. 6, pp. 942–953, 2005.

[19] H. Jin, A. Khandekar, and R. J. McEliece, "Irregular repeat-accumulate codes," in *Proc. 2nd Int. Symp. Turbo Codes & Related Topics*, Brest, France, Sept. 2000, pp. 1–8.

[20] A. Morello and V. Mignone, "DVB-S2: The second generation standard for satellite broadband services," *Proc. IEEE*, vol. 94, no. 1, pp. 210–227, Jan. 2006.

[21] M. González-López, L. Castedo, and J. Garcia-Frias, "BICM for MIMO systems using LDGM codes," in *Proceedings ICASSP'04*, Montreal, Canada, Apr. 2004.

[22] T.J.Richardson, M.A.Shokrollahi, and R.L.Urbanke, "Design of capacity-approaching irregular low-density parity-check codes," *IEEE Trans. Inform. Theory*, vol. 47, no. 2, pp. 619–637, 2001.

[23] S. ten Brink and G. Kramer, "Design of Repeat-Accumulate codes for iterative detection and decoding," *IEEE Trans. Signal Processing*, vol. 51, no. 11, pp. 2764–2772, Nov. 2003.

[24] G. Yue and X. Wang, "Optimization of Irregular Repeat Accumulate codes for MIMO systems with iterative receivers," *IEEE Trans. Wireless Commun.*, vol. 4, no. 6, pp. 2843–2855, Nov. 2005.

[25] M. González-López, F. Vázquez-Araújo, L. Castedo, and J. Garcia-Frias, "Design of Serially-Concatenated Low-Density Generator Matrix codes using EXIT charts," in *Intl. Symp. on Turbo Codes & Related Topics*, Munich, Ger., Apr. 2006.

[26] S. ten Brink, "Iterative demapping and decoding for multilevel modulation," in *Proc. Globecom '98*, 1998, pp. 579–584.

[27] X. Wang and H. V. Poor, "Iterative (turbo) soft interference cancellation and decoding for coded CDMA," *IEEE Trans. Commun.*, vol. 47, no. 7, pp. 1046–1061, July 1999.

[28] K. R. Narayanan, X. Wang, and G. Yue, "Estimating the PDF of the SIC-MMSE equalizer output and its applications in designing LDPC codes with Turbo equalization," *IEEE Trans. Wireless Commun.*, vol. 4, no. 1, pp. 278–287, Jan. 2005.

[29] M. O. Damen, H. E. Gamal, and G. Caire, "On Maximum-Likelihood detection and the search for the closest lattice point," *IEEE Trans. Inform. Theory*, vol. 49, no. 10, pp. 2389–2402, Oct. 2003.

[30] H. Vikalo, B. Hassibi, and T. Kailath, "Iterative decoding for MIMO channels via modified sphere decoding," *IEEE Trans. Wireless Commun.*, vol. 3, no. 6, pp. 2299–2311, Nov. 2004.

[31] G. Taricco and E. Biglieri, "Space-Time decoding with imperfect channel estimation," *IEEE Trans. Wireless Commun.*, vol. 4, no. 4, pp. 1874–1888, July 2005.

[32] M. González-López, J. Míguez, and L. Castedo, "Maximum likelihood turbo iterative channel estimation for space-time coded systems and its application to radio transmission in subway tunnels," *EURASIP Journal on Applied Signal Processing*, no. 5, pp. 1–13, 2004.

[33] A. P. Dempster, N. M. Laird, and D. B. Rubin, "Maximum likelihood from incomplete data via the EM algorithm," *J. Roy. Stat. Soc.*, no. 39, pp. 1–38, 1977.

[34] F.R.Kschischang, B.J.Frey, and H. Loeliger, "Factor graphs and the sum-product algorithm," *IEEE Trans. Inform. Theory*, vol. 47, no. 2, pp. 498–519, 2001.

[35] U. Fincke and M. Post, "Improved methods for calculating vectors of short length in a lattice, including a complexity analysis," *Math. Comp.*, vol. 44, pp. 463–471, Apr. 1985.

[36] W. H. Wow, "Universal lattice decoding: principle and recent advances," *Wirel. Commun. and Mob. Comput.*, vol. 3, pp. 553–559, Aug. 2003.

[37] S. Y. Chung, T. J. Richardson, and R. Urbanke, "Analysis of sum-product decoding of Low-Density Parity-Check codes using a Gaussian approximation," *IEEE Trans. Inform. Theory*, vol. 47, no. 2, pp. 657–670, Feb. 2001.

[38] S. ten Brink, "Convergence of iterative decoding," *IEE Electronics Letters*, vol. 35, no. 13, pp. 1117–1118, June 1999.

[39] ——, "Convergence behavior of iteratively decoded parallel concatenated codes," *IEEE Trans. Commun.*, vol. 49, no. 10, pp. 1727–1737, Oct. 2001.

Antennas	Modul.	Detector	$p(\%)$	$d_u^{f^1}$	$d_u^{f^2}$	$d_{p^1}^{f^2}$	Thresh (dB)	UCL	CCL
1×1	QPSK	Optimum	2%	3	6	6	2.3	1.05	1.8
2×1	QPSK	Optimum	4.5%	3	4	20	3.89	2.55	3.3
2×2	QPSK	Optimum	3%	3	5	28	1.97	1.2	1.55
2×2	16QAM	Optimum / ML 128 / EXT 32	4.5%	3	4	20	4.8	3.7	4.1
		ML 64 / EXT 16					4.9		
2×2	64QAM	ML 512/256	2%	4	5	23	7.6	6.1	6.65
		ML 128/64	2.5%	3	5	20	7.8/8.1		
		EXT 128/64/32	4%	3	4	22	7.6		
4×1	QPSK	Optimum	4.6%	3	2	18	8.5	6.25	6.7
4×2	QPSK	Optimum	2%	3	4	20	3.8	2.65	3.0
4×4	QPSK	Optimum	2%	3	5	15	1.8	1.2	1.5
4×4	16QAM	ML 512/256/128/64	2.5%	3	5	20	5.1/5.1/5.3/5.5	3.8	4.1
		EXT 256/128/64/32	3.5%	3	4	16	4.8/4.9/4.9/5.0		
4×4	64QAM	ML 256/128/64	2.5%	3	5	20	8.9/9.2/9.7	6.3	-
		EXT 128/64/32	2.5%	3	4	24	7.8/7.9/8.1		

TABLE I

DEGREE PROFILES OF RATE $1/2$ OPTIMIZED SCLDGM CODES FOR DIFFERENT MIMO CHANNELS AND DETECTORS. "THRESH" STANDS FOR THE EXIT ANALYSIS CONVERGENCE THRESHOLD. "UCL" AND "CCL" ARE, RESPECTIVELY, THE UNCONSTRAINED-INPUT AND CONSTRAINED-INPUT ERGODIC CAPACITY LIMITS.

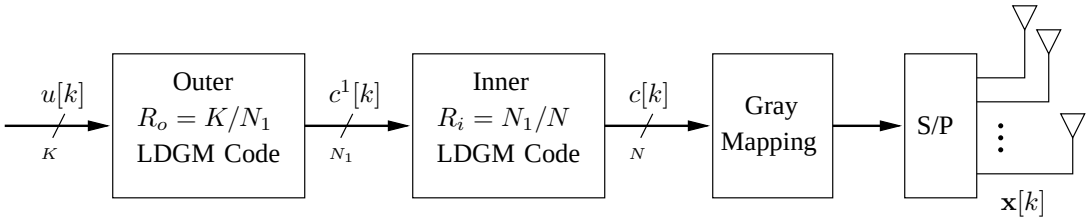

Fig. 1. Transmitter block diagram of an SCLDGM-coded MIMO system.

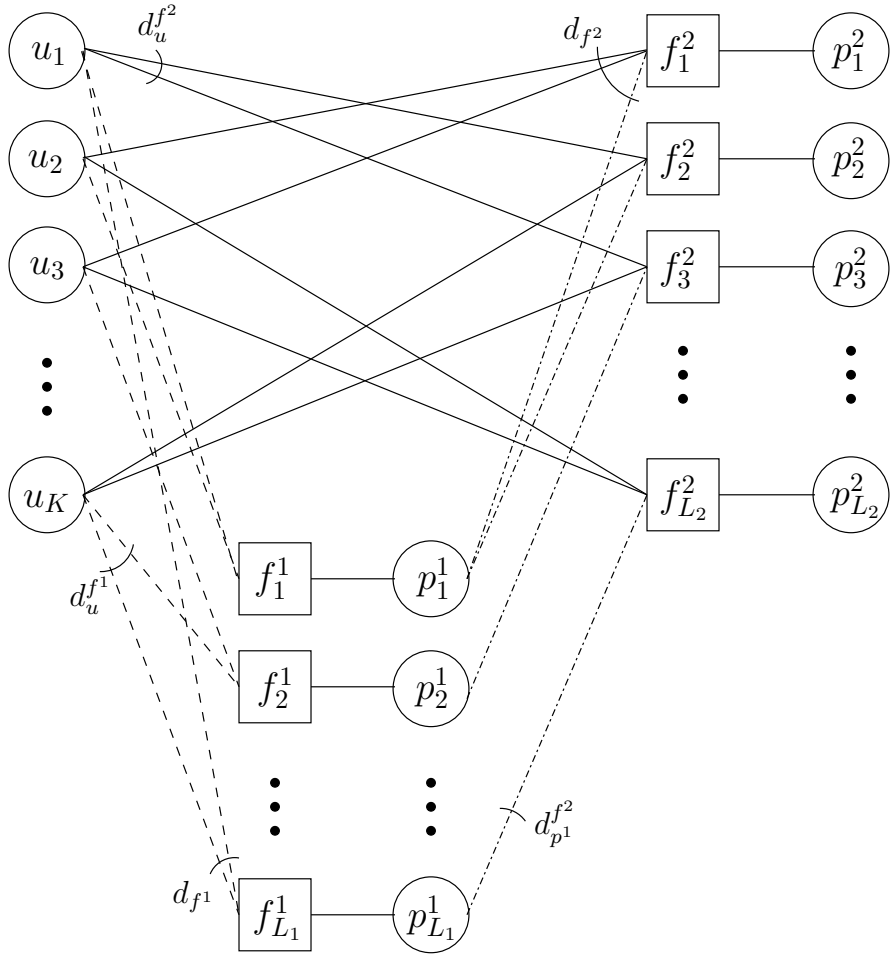

Fig. 2. Factor graph of an SCLDGM code

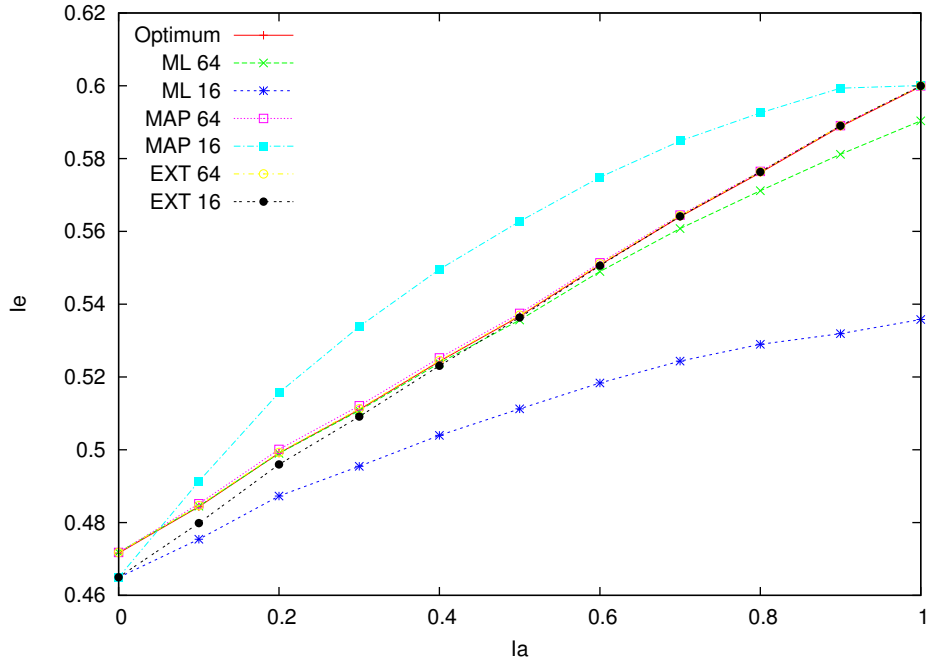

Fig. 3. EXIT characteristic of different detectors for a 4×4 QPSK MIMO channel and $E_s/N_0 = 2.0$ dB.

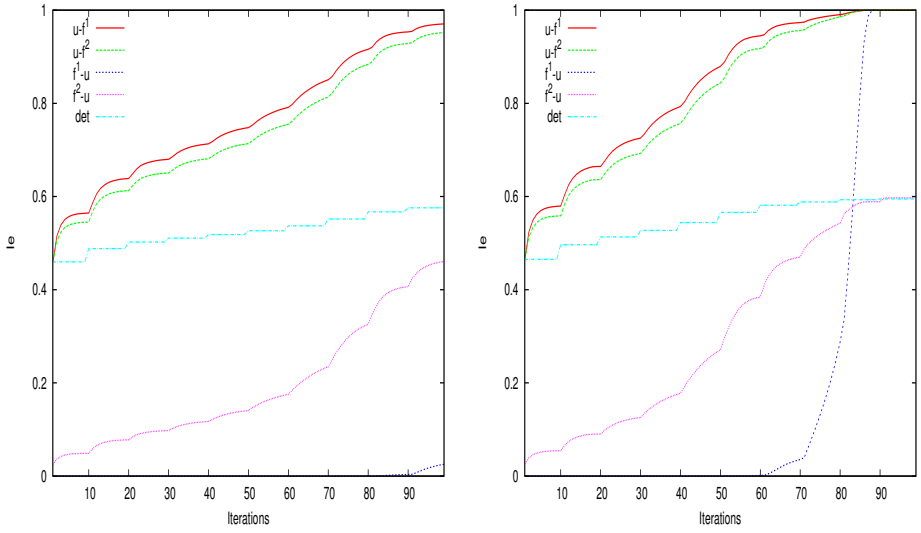

Fig. 4. Mutual information trajectories for a 4×4 QPSK optimized SCLDGM code. $E_b/N_0 = 1.75$ (left) and $E_b/N_0 = 1.80$ dB (right).

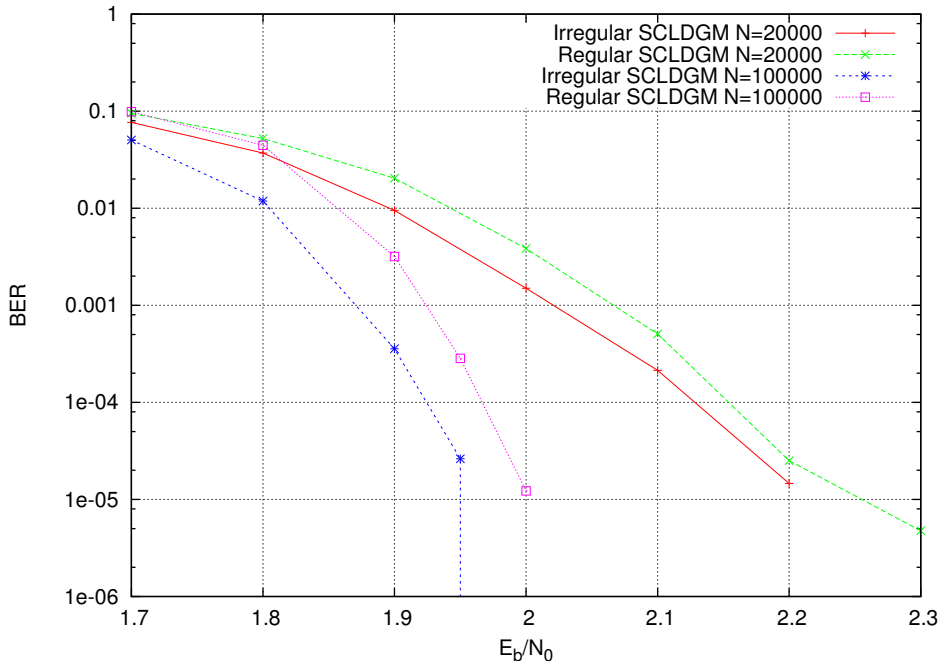

Fig. 5. Performance of rate $1/2$ regular and irregular SCLDGM codes optimized for a 4×4 QPSK MIMO channel and optimum detection. The constrained-input capacity limit is at $E_b/N_0 = 1.5$ dB whereas the convergence thresholds predicted by EXIT analysis are at $E_b/N_0 = 1.75$ (irregular) and $E_b/N_0 = 1.80$ dB (regular).

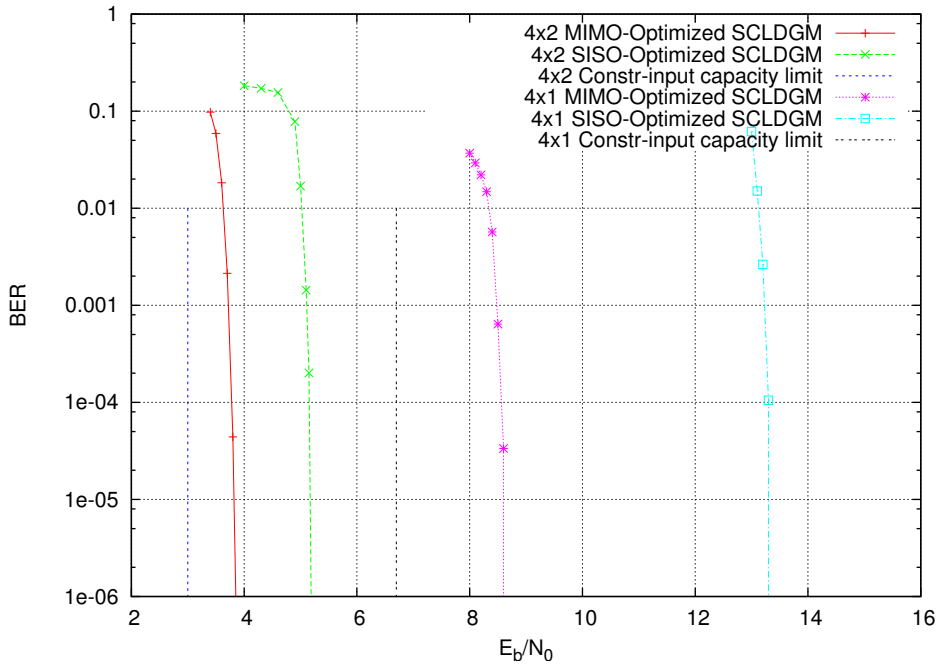

Fig. 6. Performance comparison between SISO-optimized and MIMO-optimized rate $1/2$ regular SCLDGM codes for 4×2 and 4×1 QPSK MIMO channels and optimum detection. The constrained-input capacity limit is at $E_b/N_0 = 3.0$ dB and $E_b/N_0 = 6.7$ dB, respectively.

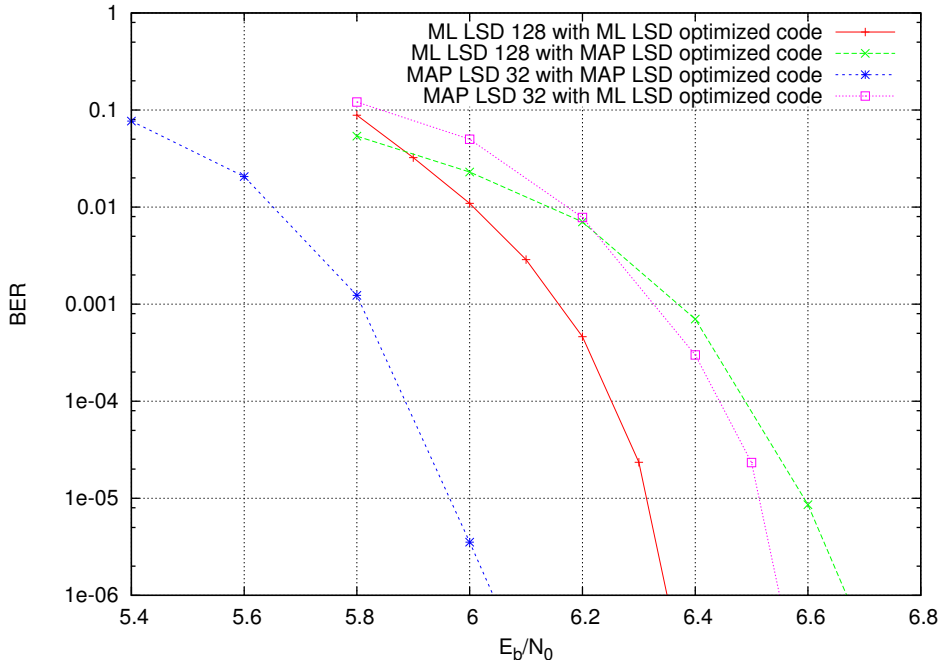

Fig. 7. Performance degradation due to mismatch between the SCLDGM code and the detector. SCLDGM codes are regular, rate $1/2$ and optimized for a 4×4 16-QAM MIMO channel and two types of LSD: ML with 128 candidates and MAP with 32 candidates.

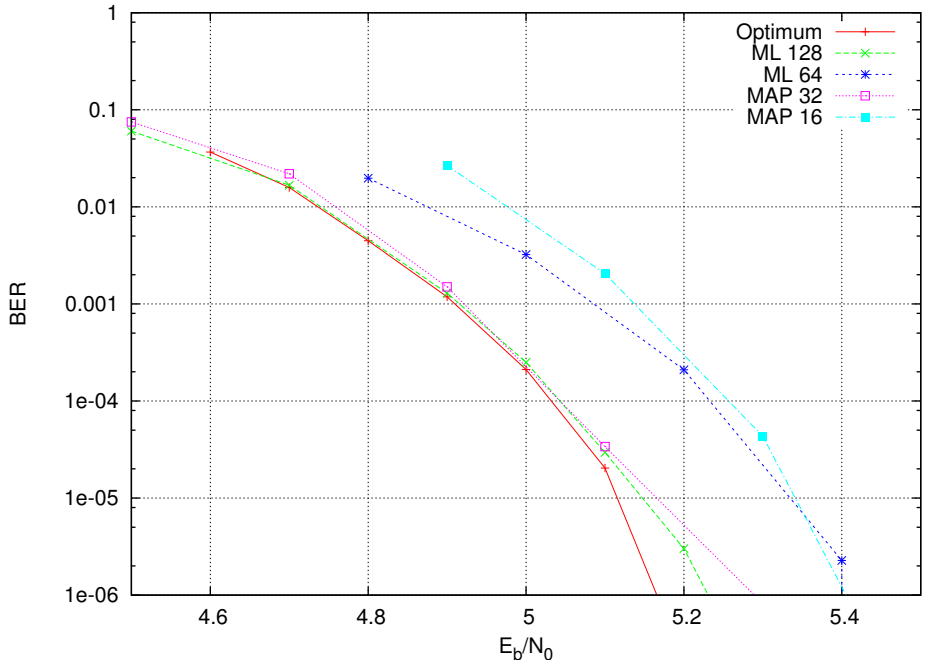

Fig. 8. Performance of rate $1/2$ regular SCLDGM codes optimized for a 2×2 16-QAM MIMO channel with different types of detectors and number of candidates. The constrained-input capacity limit is at $E_b/N_0 = 4.1$ dB.

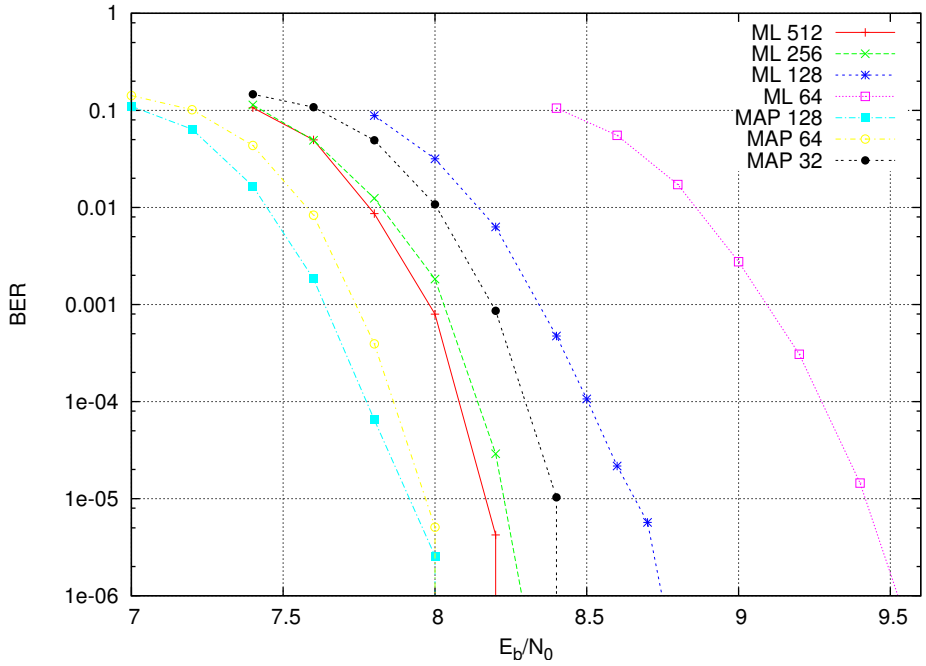

Fig. 9. Performance of rate $1/2$ regular SCLDGM codes optimized for 2×2 64-QAM MIMO channel with different types of detectors and number of candidates. The constrained-input capacity limit is at $E_b/N_0 = 6.65$ dB.

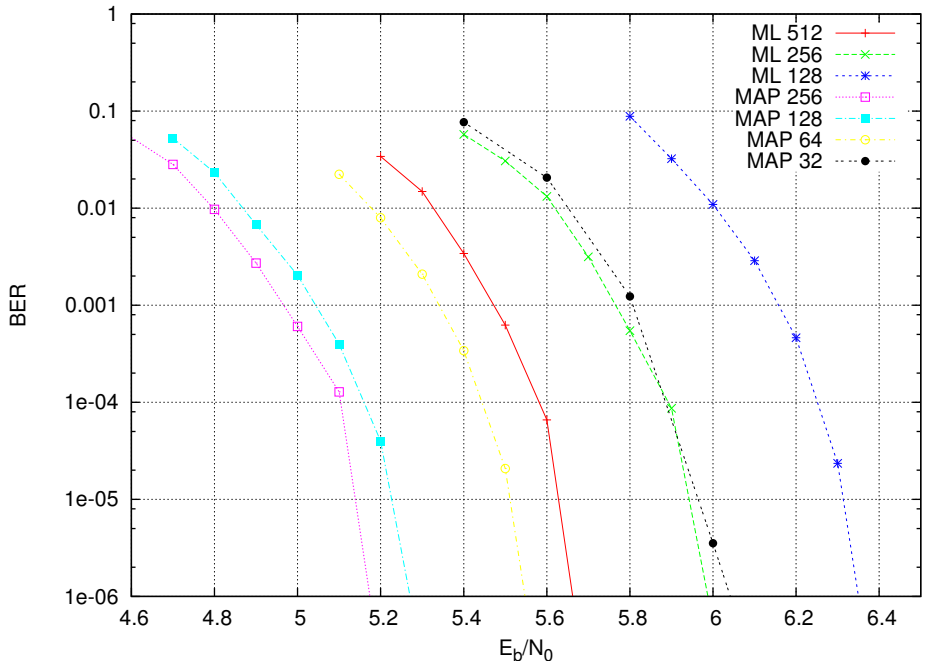

Fig. 10. Performance of rate $1/2$ regular SCLDGM codes optimized for a 4×4 16-QAM MIMO channel with different types of detectors and number of candidates. The constrained-input capacity limit is at $E_b/N_0 = 4.1$ dB.

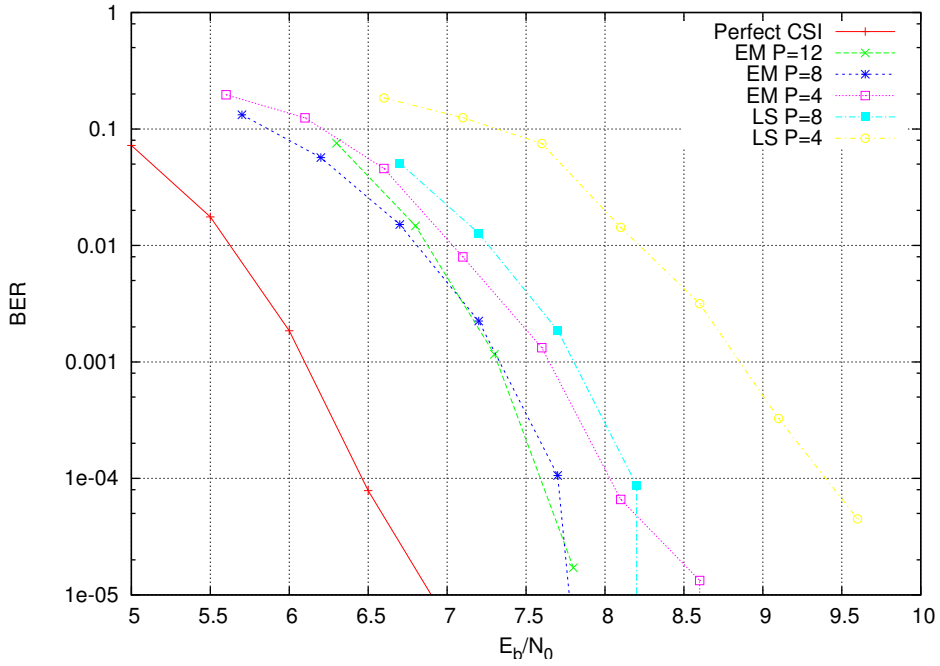

Fig. 11. Performance of the rate $1/2$ regular SCLDGM code optimized for a 4×4 16-QAM MIMO system and a MAP LSD with 64 candidates when the channel is imperfectly estimated. Two types of channel estimates are considered, Expectation Maximization (EM) and Least-Squares (LS), with different numbers of pilot symbol vectors ($P = 12$, $P = 8$ and $P = 4$).